Integrin–Cytoskeletal Interactions in Migrating Fibroblasts are Dynamic, Asymmetric, and Regulated

Christine E. Schmidt,[*‡] Alan F. Horwitz,[‡] Douglas A. Lauffenburger,[*‡] and Michael P. Sheetz[§]

[*]Department of Chemical Engineering and [‡]Department of Cell and Structural Biology, University of Illinois, Urbana, Illinois 61801; and [§]Department of Cell Biology, Duke University Medical Center, Durham, North Carolina 27710

Abstract. We have used laser optical trapping and nanometer-level motion analysis to investigate the cytoskeletal associations and surface dynamics of $\beta 1$ integrin, a cell-substrate adhesion molecule, on the dorsal surfaces of migrating fibroblast cells. A single-beam optical gradient trap (laser tweezers) was used to restrain polystyrene beads conjugated with anti-$\beta 1$ integrin mAbs and place them at desired locations on the cell exterior. This technique was used to demonstrate a spatial difference in integrin–cytoskeleton interactions in migrating cells. We found a distinct increase in the stable attachment of beads, and subsequent rearward flow, on the lamellipodia of locomoting cells compared with the retracting portions. Complementary to the enhanced linkage of integrin at the cell lamellipodium, the membrane was more deformable at the rear versus the front of moving cells while nonmotile cells did not exhibit this asymmetry in membrane architecture. Video microscopy and nanometer-precision tracking routines were used to study the surface dynamics of integrin on the lamellipodia of migrating cells by monitoring the displacements of colloidal gold particles coated with anti-$\beta 1$ integrin mAbs. Small gold aggregates were rapidly transported preferentially to the leading edge of the lamellipod where they resumed diffusion restricted along the edge. This fast transport was characterized by brief periods of directed movement ("jumps") having an instantaneous velocity of 37 ± 15 μm/min (SD), separated by periods of diffusion. In contrast, larger aggregates of gold particles and the large latex beads underwent slow, steady rearward movement (0.85 ± 0.44 μm/min) (SD) at a rate similar to that reported for other capping events and for migration of these cells. Cell lines containing mutated $\beta 1$ integrins were used to show that the cytoplasmic domain is essential for an asymmetry in attachment of integrin to the underlying cytoskeletal network and is also necessary for rapid, intermittent transport. However, enhanced membrane deformability at the cell rear does not require integrin-cytoskeletal interactions. We also demonstrated that posttranslational modifications of integrin could potentially play a role in these phenomena.

These results suggest a scheme for the role of dynamic integrin-mediated adhesive interactions in cell migration. Integrins are transported preferentially to the cell front where they form nascent adhesions. These adhesive structures grow in size and associate with the cytoskeleton that exerts a rearward force on them. Dorsal aggregates move rearward while those on the ventral side remain fixed to the substrate allowing the cell body to move forward. Detachment of the cell rear occurs by at least two modes: (a) weakened integrin-cytoskeleton interactions, potentially mediated by local modifications of linkage proteins, which lead to weakened cell–substratum interactions and (b) ripping of integrins and the highly deformable membrane from the cell body.

NUMEROUS cell types undergo directed migration, and although each cell retains distinct characteristics of its phenotype including its morphology, there are similarities in the migration of most cells. These include (a) force generation involving the cytoskeleton, (b) adhesive

contacts between the cell and its surroundings, and (c) cell polarity (Trinkaus, 1984; Singer and Kupfer, 1986; Bershadsky and Vasiliev, 1988). In this study, we are focusing on the adhesive interactions of locomoting cells.

An adhesive interaction of the cell with its substratum is an integral component of cell migration. Contacts are typically mediated by transmembrane adhesion receptors that link the internal cytoskeleton and its associated motors to extracellular surfaces. This transmembrane link allows con-

Address all correspondence to Professor Douglas A. Lauffenburger, Department of Cell & Structural Biology, 511 Morrill Hall, 505 S. Goodwin Ave., Urbana IL 61801.

tractile forces within the cell to be transmitted through adhesive structures as traction forces along a nondeformable surface (Singer and Kupfer, 1986; Heidemann et al., 1990; Wang et al., 1993). An asymmetry in traction forces between the cell front and cell rear has been proposed as necessary for net cell translocation (Trinkaus, 1984; Lackie, 1986; DiMilla et al., 1991), and it is conceivable that this asymmetry could exist at the level of the adhesion receptor interaction with the cytoskeleton.

Integrin, a transmembrane glycoprotein comprised of α and β chains, is linked between the extracellular matrix and the actin cytoskeleton through a series of intermediate proteins (Horwitz et al., 1986; Burridge et al., 1988; Otey et al., 1990) and mediates adhesion of cells to various substrata (Hynes, 1987; Ruoslahti and Pierschbacher, 1987; Buck and Horwitz, 1987; Albelda, 1990). Therefore, integrin plays a crucial role in cell migration. In nonmotile cells, $\beta 1$ integrin is localized in highly organized focal adhesions at the ends of actin stress fibers. In motile cells, integrin is found in organized, yet highly dynamic, structures (macroaggregates) that are not as closely associated with the substratum as are focal adhesions in static cells (Regen and Horwitz, 1992). These adhesions tend to remain fixed on the substratum until they reach an edge or tail where some integrin releases and moves forward, possibly to be used in new adhesive contacts at the cell front. However, there is scant information concerning the role and regulation of this surface transport of integrin in migrating cells and the nature of possible integrin cytoskeletal associations.

Although little is known about the surface dynamics of integrin in motile cells, there exist many observations on the behavior of general cell surface glycoproteins. A number of investigators have observed a rearward flow of particles and ConA-coated beads on the dorsal and ventral surfaces of migrating cells (Harris and Dunn, 1972; Dembo and Harris, 1981; Fisher et al., 1988). This phenomenon was attributed originally to membrane or lipid flow (Abercrombie et al., 1970, 1972; Bray, 1970, 1973; Edidin and Weiss, 1972; Bretscher, 1976), but there is increasing evidence that transmembrane proteins bind to the underlying moving cytoskeleton, which in turn drives particle flow on the cell surface (Sheetz et al., 1989; Kucik et al., 1990; Lee et al., 1990). Kucik et al. (1991) postulated that similar motions on the underside of the cell, in which the proteins are now attached to the substratum, could result in a forward motion of the cell. In addition to this rearward flow of large (>0.2 μm) particles and beads, Kucik et al. (1989) used nanometer-level motion analysis (Gelles et al., 1988) to demonstrate that smaller, 40-nm, ConA-coated gold beads were rapidly and intermittently transported exclusively forward on migrating fish keratocytes. Furthermore, a similar behavior was demonstrated for specific glycoproteins on neuronal growth cones (Sheetz et al., 1990). This has led to the hypothesis that these motions are possibly driven by a motor protein and that they may be the means by which the cell delivers proteins to its leading edge.

In the present study, we explored the possibility of a spatial polarity in integrin cytoskeletal associations between the lamellipodium and rear of migrating fibroblast cells. Furthermore, we investigated the dynamics and the nature of $\beta 1$ integrin supply to areas of new adhesions. To date, there exists no conclusive evidence for interactions of the α subunit

of integrin with the cytoskeleton, suggesting that this function relies predominantly with the β subunit (Solowska et al., 1989; Hayashi et al., 1990; LaFlamme et al., 1992). Therefore, to explore the important elements of integrin–cytoskeleton associations, we used NIH 3T3 mouse fibroblast cells transfected with chicken $\beta 1$ integrin $(\beta 1_c)$[1] cDNAs containing various mutations in the cytoplasmic domain. These avian $\beta 1$ integrin subunits form functional heterodimers with the native mouse $\alpha 5$ subunits, $\alpha 5_m$, and interact with the actin cytoskeleton to different extents (Hayashi et al., 1990; Reszka et al., 1992). Mutated $\beta 1_c$ integrins were monitored using nonadhesion-perturbing mAbs directed specifically against the $\beta 1_c$ subunit.

We used laser optical trapping and nanometer-precision motion analysis to investigate the interplay between cross-linked $\beta 1_c$ integrins and the dynamic cytoskeletal network in motile cells. Particles coated with anti-$\beta 1_c$ mAbs were specifically placed using a laser optical trap on the advancing and retracting portions of locomoting 3T3 cells to test the interaction of wild-type (WT) and mutant integrin with the cytoskeleton (see Kucik et al., 1991). In addition, gold particles tagged with anti-$\beta 1_c$ mAbs were allowed to interact with the dorsal surface of migrating transfected 3T3 cells. Individual and aggregated beads were tracked using video microscopy and image analysis techniques to yield information on the diffusion and directed transport of WT and mutant integrins.

We find that integrin binds to the cytoskeleton more readily at the lamellipodium compared with the rear of a migrating cell. Further, the membrane is significantly more deformable at the cell rear compared with the cell lamellipod. In addition, integrins bound by small aggregates of gold particles display rapid, intermittent motions directed preferentially to a cell edge, where they remain for extended periods of time. In contrast, integrins cross-linked by large aggregates of gold particles or by larger latex beads move slowly and steadily rearward with respect to the substratum. These findings suggest a scheme for the role of dynamic integrin-mediated adhesive interactions in cell migration.

Materials and Methods

Cell Cultures

NIH 3T3 mouse fibroblasts were cultured in high-glucose DME containing 10% calf serum (Hyclone Laboratories, Inc., Logan, UT). Cells were grown at 37°C in a 10% CO_2 incubator and passaged every 2-3 d at 1:10 dilution. NIH 3T3 cells transfected with WT and mutant chicken integrin $\beta 1$ $(\beta 1_c)$ subunit cDNAs were kindly provided by Drs. Y. Hayashi and A. Reszka (Hayashi et al., 1990; Reszka et al., 1992). The transfectants were cultured in the above media supplemented with 250 μg/ml geneticin or G418 sulfate (GIBCO BRL, Gaithersburg, MD).

The particular mutant constructs used were: 765t, R765I, S790M, S790D, Y788F, and Y788E (Table I). The 765t cells express $\beta 1_c$ integrin that has a truncated cytoplasmic domain and does not interact with the cytoskeleton, as determined by its inability to localize in adhesion plaques. R765I cells express integrin that is altered at a residue that has not been previously identified as critical for integrin cytoskeletal interactions based on the same assay. The S790M/D and Y788F/E integrin constructs contain amino acid substitutions at residues previously shown to be critical for regu-

---

lation of cytoskeletal interactions (Hayashi et al., 1990; Reszka et al., 1992) by phosphorylation (Hirst et al., 1986; Tapley et al., 1989; Horvath et al., 1990). S790M and Y788F substitutions, which cannot be phosphorylated, localize normally in focal adhesions. On the other hand, S790D and Y788E mutations contain negatively charged amino acids that mimic the phosphorylated states of these residues, and subsequently, have impaired focal contact localization (Hayashi et al., 1990; Reszka et al., 1992).

Matrix Proteins and Antibodies

Laminin and fibronectin were isolated from murine Engelbreth-Holm-Swarm tumors and human blood plasma, respectively, as described previously (Ruoslahti et al., 1982; Rupert et al., 1982). ES66-8 rat hybridoma cells were generously provided by Dr. Kenneth Yamada (National Institutes of Health [NIH], Bethesda, MD). ES66 is a nonadhesion perturbing mAb directed against the chicken $\beta1$ integrin (Duband et al., 1988). Antibody was purified from hybridoma supernatants by ammonium sulfate precipitation, followed by anion exchange chromatography (Duband et al., 1988).

Bead Preparation

ES66 mAb was either adsorbed to 40-nm-diameter colloidal gold particles or chemically conjugated via a carbodiimide linkage to the surfaces of activated 0.5-μm-diameter polystyrene (latex) beads. For gold bead preparations, ES66 mAb was diluted to a final concentration of 0.1 mg/ml in 0.5 ml of calcium and magnesium-free PBS (CMF-PBS). 0.5 ml of 40-nm (diameter) gold bead suspension (EY Laboratories Inc., San Mateo, CA) was added to the antibody solution and incubated on ice for 5 min. The beads were washed three times with 5 mg/ml BSA in CMF-PBS by centrifugation at 20,000 rpm and 4°C for 10 min in a Beckman TL-100 ultracentrifuge using a TLS-55 swinging bucket rotor (Beckman Instruments, Inc., Palo Alto, CA). The final bead pellet was resuspended in 50 μl of microscopy media (high-glucose DME without phenol red containing 10% calf serum and supplemented with 0.02 M Hepes) and sonicated to break up aggregates. The beads were diluted 1:3 in microscopy media and sonicated just before their use.

For latex bead preparations, ES66 mAb was prepared at a concentration of 2 mg/ml in 100 μl of 0.5% BSA in CMF-PBS. 50 μl of 0.5-μm Covaspheres® MX reagent (Duke Scientific Corp., Palo Alto, CA) was added to the mAb solution and allowed to incubate overnight at 4°C. The bead solution was diluted 1:1000 in microscopy media then sonicated before being added to the cells.

To ensure that ES66-coated beads properly recognized $\beta1_c$ integrin, integrin localization was monitored using immunofluorescent techniques (data not shown). 3T3 WT cells plated on fibronectin and laminin were stained for integrin localization with ES66 antibody (mAb) as well as with ES66 coupled to the gold and the latex beads. Secondary Abs tagged with FITC were used to visualize the ES66 primary Ab. Normal ventral surface focal contact staining patterns were seen for all cases on fibronectin. Similarly organized, yet more fibrillar, integrin aggregates were observed for all cases on laminin. There were no differences in localization patterns for the ES66 Ab coupled to either the gold or latex beads compared with the unconjugated Ab. These data suggest that coupling of the ES66 mAb to the beads does not interfere with the Ab's ability to recognize integrin.

Cell Preparation for Microscopy

No. 1 glass coverslips, 22 mm², (VWR, San Francisco, CA) were cleaned by soaking in 20% HNO₃ for 30 min, followed by rinsing in distilled water overnight, and drying with acetone. The coverslips were silanized by exposure to hexamethyldisilazane vapor (Eastman Kodak Co., Rochester, NY) for 30 min at 200°C (Regen and Horwitz, 1992). This treatment blocks charged groups on the glass, thereby enhancing matrix protein adsorption and preventing nonspecific adhesion of cells to the coverslip. Coverslips were sterilized by soaking in 70% ethanol and drying in a sterile laminar flow hood.

Sterile coverslips were placed in 35-mm cell culture dishes and coated with 40 μg/ml of laminin in CMF-PBS overnight at 4°C. Cells were rinsed once with 0.02% EDTA in CMF-PBS and then treated with 0.25% trypsin (GIBCO BRL) in CMF-PBS for 2-5 min at 37°C. Cells were suspended in 5 ml of the appropriate cell media, then seeded at low density onto a laminin-coated coverslip. The cells were incubated at 37°C in 10% CO₂. After 4 h, the cells were rinsed three times with warmed microscopy media. The coverslip containing the cells was then mounted on an aluminum coverslip holder using vacuum grease. 20 μl of the appropriate bead solution diluted in warmed microscopy medium was added to the cells, and then a

second 22-mm², No. 1 glass coverslip was mounted on top. The unit was sealed at the corners using hot wax.

For nonmotile cell controls, coverslips were coated overnight at 4°C with 40 μg/ml of fibronectin, which promotes stronger cell adhesion. Cells were treated identically to the method described above, except that they were incubated for 4 h in serum-free media (cell media without calf serum, supplemented with 2% BSA). Serum-free media promoted extensive cell spreading and inhibited cell migration.

Video Microscopy

Cells were viewed by high-magnification, video-enhanced differential interference contrast (DIC) microscopy (IM-35; Zeiss, Oberkochen, Germany) with a fiber optic illuminator. The microscope stage was maintained at 37°C using an air current incubator. Images were collected with a video camera (VE1000; Dage-MTI Inc., Wabash, MI) and stored on one-half-inch s-VHS videotape using an s-VHS VCR (AG-7300; Panasonic, Secaucus, NJ). Images were digitized at video rate, 30 Hz, from the videotape using a series 151 Image Processor (Imaging Technology, Inc., Woburn, MA), an IBM PC/AT-compatible computer (Zenith Z386/25 with 150 Mb hard disk), and a real time storage system (model 8300; Applied Memory Technology, Tustin, CA). A time-base corrector (FA-300; FOR-A, Boston, MA) was used to synchronize the video image timing signal prior to digitization by the image processor.

Selection of Motile and Nonmotile Cells

Locomoting cells were selected for analysis based on a characteristic polar morphology consisting of an actively spreading lamella and a distinct retracting edge (Regen and Horwitz, 1992). Nonmotile cells, grown on fibronectin and without serum, were characterized by their lack of actively spreading and retracting regions. Static cells were also distinguished by a "pinned-out" appearance in which multiple vertices, distributed randomly around the cell periphery, were in contact with the substratum. Therefore, in trapping experiments "front" and "rear" on nonmotile cells were assigned arbitrarily. Cells were viewed at a magnification of 60 through the microscope eye piece, so that whole cell morphologies and migration patterns were easily identified and noted. However, only small, highly magnified portions of the cell could be recorded onto videotape for particle trapping and tracking analyses.

The retracting region (tail) differed significantly from one cell to the next. Some cells had elongated tails, while others had shorter tails with little membrane behind the cell. Laser trapping experiments conducted on the cell rear were performed at random locations along the length of the tail and for a wide range of tail morphologies; no significant differences were apparent. Latex trapping experiments conducted at the cell front were performed on the lamellipodium (3-5 μm from leading edge), which is easily detected with DIC microscopy at a magnification of 60. Gold particle tracking experiments were conducted exclusively on the organelle-free lamellipodium, but not on the thicker cell rear because the particles could not be distinguished from the organelles.

Nanometer-precision Analysis of Bead Position

Positions of the selected gold beads in the digitized images were determined by the computer and image processor for each video frame using the cross-correlation method of Gelles at al. (1988). In a few cases, the centroid of the bright portion of the DIC image was determined from the weighted pixel intensity without using cross-correlation analysis. For each moving bead analyzed, a second bead attached directly to the glass coverslip was also tracked and used as a stationary reference point. Beads were tracked at video rate, 30 frames/s, over a total time of 90 s. We determined the accuracy of tracking 40-nm gold particles using cross-correlation analysis to be ±(5-10) nm and the accuracy for centroid tracking to be ±(15-25) nm.

Distinguishing Directed Transport versus Diffusion

Directed versus diffusive motion was determined statistically. The displacements that each bead traversed for the total tracking time of 90 s were determined from images of the cells and compared with the distance predicted for a purely diffusing particle. The statistical probability that a particle undergoing a random walk will diffuse to a distance between x and $x + dx$ is described by the equation

$$P(x)dx = 1/(4\pi Dt)^{1/2}\exp(-x^2/4Dt)dx$$

(Berg, 1983). Integrating this equation from x to ∞ yields the probability that a particle has diffused a distance greater than the actual displacement measured, x, where $P(x)$ is the error function, $\text{erf}(x/\sqrt{4Dt})$. To evaluate this probability, t is the time interval over which x is measured and D is the two-dimensional diffusivity determined from a plot of mean–square displacement (MSD) vs. time (see below). A low value for $P(x)$ suggests that some active process in addition to diffusion contributes to the large displacement of the integrin-bound bead. A cut off for $P(x)$ of 0.05 was used. In other words, particle displacements having a probability of 5% or more as resulting from diffusion $[P(x) \geq 0.05]$ were scored as diffusive, and those with $P(x) < 0.05$ were considered directed.

As a second check to distinguish directed behavior from pure diffusion, plots of parallel MSD vs. time interval (Sheetz et al., 1989) were constructed for each particle path. Parallel MSD data were generated by determining the displacement of the bead parallel to the general direction of motion for the bead, as determined by a least squares fit of the (x, y) data for the bead. A linear parallel MSD vs. time relationship is indicative of pure diffusion, $\text{MSD} = 2Dt$, and a nonlinear relationship with an upward curvature is characteristic of a particle undergoing both directed motion and diffusion, $\text{MSD} = 2Dt + (vt)^2$. Therefore, parallel MSD plots were constructed for each particle track and fit using the method of least squares to either a first or second order polynomial. These fits were subsequently used to confirm whether a bead exhibited directed or diffusive character, based on the relative contributions of the two terms.

Values for the velocity of directed motion, v, and the bead diffusivity, D, were extracted from plots of parallel and two-dimensional MSD vs. time plots. The average velocity for directed motion, v, was obtained from a second order polynomial fit of the parallel MSD data to the function $\text{MSD} = 2Dt + (vt)^2$. Since this relationship assumes a constant velocity imposed on the particle, the reported v is an average, with the instantaneous velocity, v_i, of individual jumps being higher. The diffusion coefficient, D, was determined from plots of two-dimensional MSD versus time, $\text{MSD} = 4Dt + (vt)^2$ and $\text{MSD} = 4Dt$, to yield a representative diffusivity in all directions.

Laser Optical Trapping

Details of the construction and calibration of the laser optical trap have been described previously (Kuo et al., 1991). The laser trap consists of a polarized beam from a 1W TEM_{00}-mode near-infrared (1064 nm) laser (model C-95; CVI Corp., Albuquerque, NM) that is passed through a 3× beam expander (CVI Corp.) then focused through an 80-mm focal length achromat lens (Melles Griot, Irvine, CA) into the epifluorescence port of the Zeiss IM-35 microscope. Other investigators have demonstrated that use of low intensity levels (<250 mW) of infrared light produce negligible damage to cells (Ashkin et al., 1987; Kucik et al., 1991).

Polystyrene beads coated with anti-integrin mAbs were trapped with ~150 mW of laser light from solution and held on either the front lamellipodium or rear cell surface for 10 s to allow for interaction of the Abs on the bead with integrin in the cell membrane. The beads were consistently placed within ~2–3 μm of either the advancing or retracting edge. After release, the trap was subsequently used to classify the behavior of the underlying integrin. There were two major classes, one being negative encounters and the other encounters leading to membrane association. The latter class could be further subclassified into three categories: cytoskeletal attached, tethered, and membrane attached. Beads that diffused rapidly away from the cell surface upon release from the trap were defined as negative encounters. If the bead remained attached to the cell surface but could not be pulled by the optical tweezers, integrin was considered as "cytoskeletal attached" (Kucik at al., 1991). On the other hand, if the bead diffused in the membrane and could be pulled around within the membrane using the optical tweezers, then it was counted as "membrane attached." This movement indicates that the integrin bound by the bead was not restricted by the underlying cytoskeleton. Many beads would elastically recoil to the cell surface upon manipulation in the vertical direction (z-axis) with the laser tweezers, whereas manipulation in horizontal directions (x–y plane) exhibited movement with little apparent restraint. These elastic interactions were scored as "tethers." Tethers have been shown previously to form from cell membranes as well as from pure lipid bilayers, indicating that cytoskeletal components are not necessary for their formation (Hochmuth et al., 1982; Waugh, 1982; Ashkin and Dziedzic, 1989). The tethers that we encountered were usually small and not visible by DIC microscopy, consistent with previous work showing that tethers pulled from red blood cell membranes can be as small as 15 nm in diameter (Hochmuth et al., 1982).

Trapping results are reported as a percentage of the total number of positive cell surface interactions; i.e., the sum of cytoskeletal attached, mem-

brane bound, and tethered. This procedure removes the effects of different surface expression levels for the various integrin transfectants and also eliminates operational uncertainty in controlling the z-axis position of the latex bead with the optical tweezers. In general, contact of the bead with the cell surface was easily detected by a slight displacement of the bead in the x-y plane. However, beads that were not lowered sufficiently on the cell surface, and could not make contact (negative encounters), were not included in the reported results.

Uncertainty Calculations and Measures of Statistical Significance

The 95% confidence limits for percentages were calculated by fitting the data for each proportion to a binomial expression as described by Croxton (1958). This exact method for determining statistical uncertainties accounts for the deviation between the discontinuous data distribution for small sample sizes and the continuous normal distribution. The standard deviation for each proportion was calculated for a binomial proportion distribution as $\sqrt{pq/n}$, where p is the proportion of occurrences in a population, q is the proportion of nonoccurrences ($q = 1 - p$), and n is the number of items in a sample (Croxton, 1958; Wagner, 1992).

The statistical significance between two population proportions was determined at the 0.05 level by first assuming that the values were from the same population. The estimated standard error of the difference between the proportions was determined as

$$\sigma_{P_1-P_2} = \sqrt{\bar{p}\bar{q}/n_1 + \bar{p}\bar{q}/n_2},$$

where $\bar{p}$ is a weighted average of the proportion of occurrences for the two samples,

$$\bar{p} = (p_1 n_1 + p_2 n_2)/(n_1 + n_2),$$

and

$$\bar{q} = 1 - \bar{p}.$$

The ratio of the observed difference between the two population proportions to the estimated standard error,

$$(p_1 - p_2)/\sigma_{P_1-P_2},$$

was evaluated by referring to the normal curve (Croxton, 1958). At the 0.05 level, a value for this ratio of 1.96 or greater indicates that the two proportions represent distinct populations with 95% confidence.

Statistical significances between population means were determined similarly to those for proportions. The ratio of the observed difference between the means to the standard error is given as

$$(\bar{x}_1 - \bar{x}_2)/\sqrt{\sigma_1^2/n_1 + \sigma_2^2/n_2}$$

and was evaluated at the 0.05 level using the normal curve.

The uncertainties in front and rear cytoskeletal attachment were also determined based on levels of nonspecific binding of ES66-coated latex beads to untransfected 3T3 cells. Latex beads attached to the cytoskeleton at the front of untransfected 3T3 cells 6% of the time, to the membrane 27% of the time, and as tethers 9% of the time. Nonspecific binding to the rear of control cells was 7% for cytoskeleton binding, 44% for membrane attachment, and 7% for tether formation. These values were used to determine the overall uncertainty in the proportion of cytoskeletal attachments.

Results

$\beta 1$ Integrin Attaches Asymmetrically to the Cytoskeleton of Motile Cells

Net unidirectional locomotion conceivably involves an asymmetry of adhesion strength between the cell front and the cell rear, which could likely be regulated at the level of integrin interaction with the cytoskeleton. We used laser optical trapping and mouse fibroblasts transfected with WT chicken $\beta 1$ integrin to investigate the possibility of a spatial polarity in $\beta 1_c$ integrin cytoskeletal associations between the cell lamellipodium and cell rear.

Laser tweezers were used to place polystyrene beads

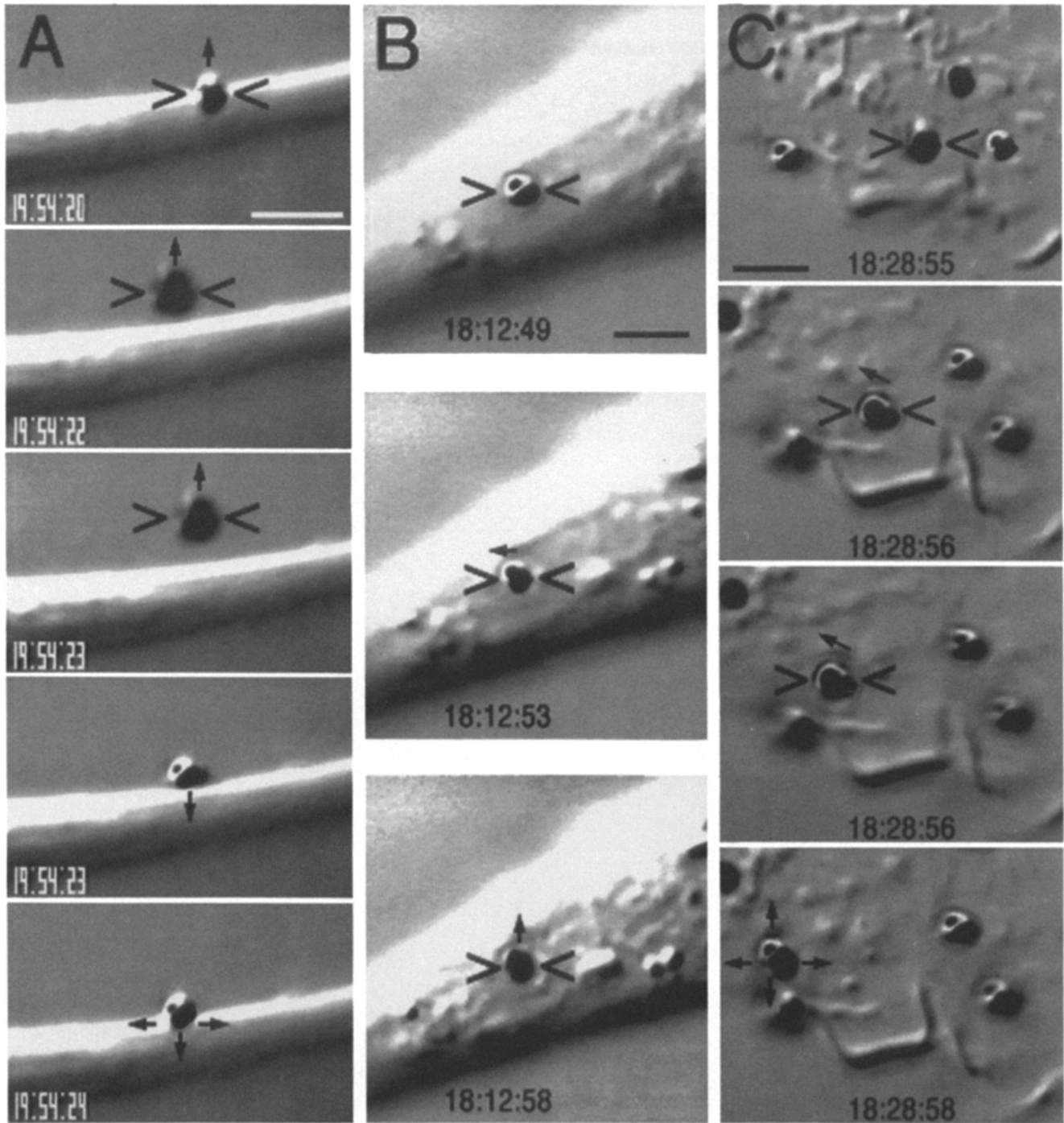*Figure 1.* Comparison of tethering (*A*), cytoskeletal (*B*), and membrane (*C*) interactions of latex beads bound to integrin. 0.5-μm latex beads coated with nonadhesion perturbing anti-β1$_c$ integrin mAb, ES66, were trapped from solution using laser optical tweezers and held on the dorsal surface of the cell front (lamellipod) or rear for 10 s. After release, the trap was used to manipulate the bead. In *A*, a "tethering" interaction, the trap (indicated by *carets*) moves the bead away from the surface of the cell rear (*upward arrows*) before the bead snaps out of the trap and recoils (*downward arrow*) to the cell surface where it resumes diffusive motion (shown as *three arrows*). The bead is held to the surface by a small membrane tether which is not visible by DIC microscopy. In *B*, a "cytoskeletal" interaction, the laser trap is unable to move the ES66-coated bead (direction of force indicated by arrows) on the cell rear surface, suggesting a stable linkage to the cell cytoskeleton. In *C*, a "membrane" interaction, the trap is used to move the membrane bound bead upward to the left on the lamellipod of the cell, indicating that the integrin is not attached to the cytoskeletal network. When not trapped, the bead diffuses on the cell surface (shown as *four arrows*). Bars, 3 μm.
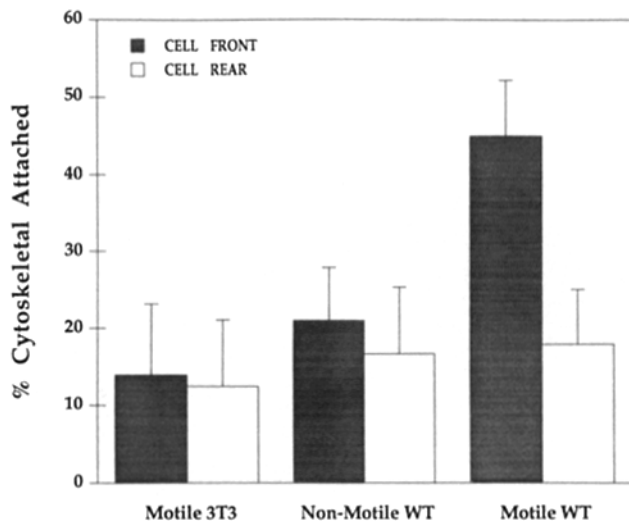
Figure 2. Front (■) versus rear (□) cytoskeletal attachment of integrin in motile and nonmotile 3T3 fibroblasts. 0.5-μm latex beads coated with the ES66 anti-$\beta1_c$ mAb were trapped using the laser trap and held on the cell surface for 10 s. After release, the bead was scored as either a negative encounter, membrane attached, cytoskeletal associated, or tethered (see Fig. 1). Locomoting cells were selected based on a polar morphology consisting of an actively spreading lamella and a distinct retracting edge. On nonmotile cells "front" and "rear" regions were assigned arbitrarily (see Materials and Methods). Motile WT cells (3T3 cells transfected with WT $\beta1_c$) display an enhanced cytoskeletal association of WT integrin at the cell front. On the other hand, nonmotile WT cells do not exhibit any asymmetry in cytoskeletal attachment. The percentage of cytoskeletal-attached beads was calculated as the ratio of cytoskeletal-attached beads relative to n, the sum of cytoskeletal attached, membrane attached, and tethered. The percentage of negative encounters varied between 30 and 50%. Values for n: untransfected 3T3, 14 (front) and 16 (rear); nonmotile 3T3 WT, 33 (front) and 18 (rear); and motile 3T3 WT, 44 (front) and 28 (rear). The error bars represent standard deviations as described in Materials and Methods. These results indicate that the spatial asymmetry in binding of integrin to the cell cytoskeleton is a phenomenon unique to moving cells.

coated with an anti-integrin mAb either on the lamellipodium or rear of migrating WT and untransfected 3T3 cells. On nonmotile cells, "front" and "rear" regions were assigned arbitrarily. Each bead was held on the surface for 10 s and then scored as either a negative encounter, cytoskeletal attached, membrane attached, or as tethered, based on further manipulation with the trap. Beads that diffused away from the cell surface upon release from the trap were scored as negative encounters. Surface-bound beads that could not be moved within the membrane by the trap were scored as cytoskeletal attached, while those that could be manipulated were scored as membrane attached or as tethers for elastic interactions. The distinction between tethering, cytoskeletal attachment and membrane bound is illustrated in Fig. 1.

Trapping experiments demonstrated a substantial increase ($P < 0.02$) in the probability of cytoskeletal binding to the lamellipodium versus the rear of motile cells containing WT chicken $\beta1$ integrin (Fig. 2). Cytoskeletal binding levels at the rear of these cells were indistinguishable from nonspecific levels of binding to untransfected 3T3 cells. This enhancement of cytoskeletal associations at the cell lamellipodium is characteristic of migrating cells, since nonmotile WT cells did not display any spatial differences in cytoskeletal attachment of integrin. In fact, cytoskeletal binding of mAb-coated beads to nonmotile WT cells was virtually identical to control levels. Beads that bound to the cell via cytoskeletal linkages were observed to move centripetally toward the nuclear region at a rate of ∼0.5-1 μm/min.

Asymmetric Attachment Requires Sequences in the β1 Cytoplasmic Domain

To explore further the cytoskeletal interactions of integrin, identical trapping experiments were conducted with 3T3 cell lines transfected with various chicken $\beta1$ integrin cDNAs mutated in the cytoplasmic domain. The mutants utilized were 765t, R765I, S790M, S790D, Y788F, and Y788E (Table I). The 765t $\beta1_c$ integrin is truncated in its cytoplasmic domain and does not localize to focal adhesions whereas R765I integrin localizes normally, as assayed by Reszka et al.

Table I. Integrin β1 Cytoplasmic Domain Mutants

Mutant	Amino acid sequence of cytoplasmic domain				
	760	770	780	790	800
WT	WKLLMIIHDRREFAKFEKEKHNAKWDTGENPIYKSAVTTVVNPKYEGK				
R765I	. . . . ● . . . . . I . . . . ● . . . . ● . . . . ● . . . . ● . . .				
765t	. . . . ●				
S790M	. . . . ● . . . . ● . . . . ● . . . . M . . . . ● . . .				
S790D	. . . . ● . . . . ● . . . . ● . . . . D . . . . ● . . .				
Y788F	. . . . ● . . . . ● . . . . ● . . . . F . ● . . . . ● . . .				
Y788E	. . . . ● . . . . ● . . . . ● . . . . E . ● . . . . ● . . .				

```
|————————|  |————————▶
Membrane   Cytoplasmic
```

Mouse NIH 3T3 fibroblasts were transfected with various constructs encoding chicken $\beta1$ integrin ($\beta1_c$). 765t is a cytoplasmic domain truncation mutation that cannot interact with the cytoskeleton while the R765I construct localizes normally to focal adhesions. The S790M/D and Y788F/E integrin constructs contain amino acid substitutions at residues previously shown to be crucial for regulation of cytoskeletal interactions (Hayashi et al., 1990; Reszka et al., 1992) by phosphorylation (Hirst et al., 1986; Tapley et al., 1989; Horvath et al., 1990). S790M and Y788F localize normally to adhesion plaques while S790D and Y788E are impaired in their localization.

(. . .) identical amino acid residues; (●) symbol used to aid in lining up the sequences.

(1992). S790M and Y788F substitutions exhibit wild-type focal contact staining patterns while S790D and Y788E mutations show impaired localization in focal adhesions (Reszka et al., 1992).

Table II summarizes the percentages of cytoskeletal attachment to the lamellipodia and retracting edges of the various motile integrin mutants. With one exception (S790M), there is a correlation between localization to focal adhesions in static cells (Reszka et al., 1992) and differential cytoskeletal linkage between the advancing and retracting portions of the migrating cell, indicating a requirement for the integrin cytoplasmic domain. For all integrins showing normal localization in focal contacts, binding to the cytoskeleton at the cell lamellipodium is significantly higher ($P < 0.05$) than attachment at the cell rear. This correlation holds for the truncation mutant as well as for the substitution mutants at potential phosphorylation sites (tyrosine 788 and serine 790). Although Y788E and S790D integrins appear to show a reversal in the front-to-rear polarity in cytoskeletal linkage, this is not statistically significant with the number of trials we have performed.

S790M does not display wild-type behavior in the trapping experiments although it has been reported to localize normally in focal adhesions (Reszka et al., 1992). The front/rear asymmetry for S790M is not as large as the others, suggesting that S790M is only partially impaired in its ability to bind to the cytoskeleton at the lamellipodium of cells. This may be due to the nonconservative substitution of serine by methionine. However, it is interesting that all of the point mutations in Reszka et al. (1992), including those used here, exhibited only partially impaired focal adhesion localization whereas the 765t mutant was completely impaired. In contrast, both of the point mutations used in this study yielded results identical to the 765t mutant in our assay. Therefore, our latex bead trapping assay appears to be more sensitive than the focal contact localization assay and may also reflect differences in the nature of the cytoskeletal linkage probed.

In addition, although R765I integrin displays wild-type front vs. rear asymmetry for cytoskeletal binding, the absolute values for attachment to the lamellipodium and rear are 44 and 27% lower, respectively, compared with WT. The cause of this discrepancy is uncertain at present. For the front vs. rear cytoskeletal attachment of R765I we obtained a P value just under the 0.05 level based on a statistical analysis. We also estimated the uncertainty in lamellipodium and rear cytoskeletal attachment based on levels of nonspecific binding of ES66-coated latex beads to untransfected 3T3 cells (see Materials and Methods). This analysis resulted in a significant difference ($P < 0.01$) between cytoskeletal binding to the front vs. the rear of the R765I cell, and the average of the nonspecific and statistical uncertainties is reported in Table II. The two uncertainties are not additive since they are not necessarily independent of each other. For the remainder of the receptor types, the nonspecific error analysis was consistent with our statistical approach.

Membrane of Motile Cells is More Deformable at the Cell Rear

The laser optical tweezers studies often detected tethering interactions of anti-$\beta 1_c$ integrin mAb-coated beads with the cell surface. In our experiments, tethering is the ability to
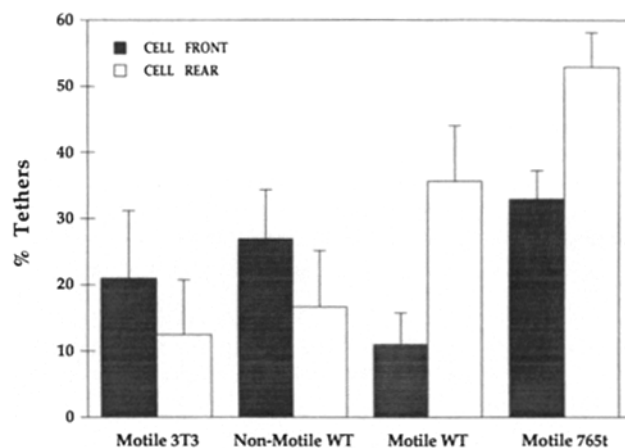

Figure 3. Front versus rear tethering of integrin on motile and nonmotile 3T3 $\beta 1_c$ integrin transfectants. 0.5-μm latex beads coated with the ES66 anti-$\beta 1_c$ mAb were trapped from solution using the laser trap and held on the cell surface for 10 s. After release, the bead was scored as either a negative encounter, membrane attached, cytoskeletal associated, or tethered. Both motile WT cells and motile cells containing the $\beta 1$ integrin cytoplasmic domain truncation, 765t, show a significant enhancement of tether formation at the rear of the cell. The other motile integrin mutants behaved similarly (data not shown). Nonmotile WT cells did not deviate significantly from nonspecific interactions on untransfected 3T3 cells. The percentage of tether formation was calculated as the ratio of the number of tethered beads relative to n, the sum of cytoskeletal attached, membrane attached, and tethered. The level of negative encounters is similar to that discussed in Fig. 2. Values for n: untransfected 3T3, 14 (front) and 16 (rear); nonmotile 3T3 WT, 33 (front) and 18 (rear); motile 3T3 WT, 44 (front) and 28 (rear); and motile 765t, 119 (front) and 87 (rear). The error bars were calculated for proportions as described in Materials and Methods. These data imply that enhanced tethering, or increased membrane deformability, at the cell rear is not a cytoskeletal event but rather a general property of migrating cells.

Table II. Spatial Asymmetry of $\beta 1$ Integrin Linkage to the Cytoskeleton Requires Sequences in the Cytoplasmic Domain

Receptor type	Percent cytoskeletal attached*				Front/ rear ratio‡	Significance§
	Front	n	Rear	n		
WT	45 ± 7.2	44	18 ± 7.1	28	2.54	P = 0.008
R765I	25 ± 4.5	69	13 ± 3.6	62	1.91	P = 0.038
765t	12 ± 3.0	119	13 ± 3.6	87	0.93	—
S790M	22 ± 7.1	32	17 ± 6.8	30	1.31	—
S790D	11 ± 5.3	36	21 ± 7.4	28	0.52	—
Y788F	40 ± 6.7	50	18 ± 5.7	45	2.25	P = 0.012
Y788E	14 ± 6.6	28	27 ± 8.9	22	0.52	—

These data suggest that stable interactions of integrin-bound beads with the cell surface, scored as cytoskeletal attached, are indeed cytoskeletal associations that require sequences in the $\beta 1$ integrin cytoplasmic domain.
* Percent cytoskeletal attached is expressed as the ratio of cytoskeletal binding relative to the total beads bound to the cell (n), summing cytoskeletal attached, membrane attached, and tethered. The reported error represents the standard deviation calculated for proportions as described in Materials and Methods.
‡ The front/rear ratio is the ratio of the beads bound as percent cytoskeletal at the cell front to those bound as percent cytoskeletal at the cell rear.
§ Significance of the differences between percent cytoskeletal attached at the front and rear, expressed as the probability, P, that the two values are the same. P was calculated using a t test for proportions as described in Materials and Methods.

stretch the membrane attached to a trapped bead (see Fig. 1). This has been described previously in other systems (Hochmuth et al., 1982; Waugh, 1982; Ashkin and Dziedzic, 1989). Note that the membrane tether in Fig. 1 is small and not visible by DIC microscopy, which is consistent with previous reports of tethers as small as 15 nm (Hochmuth et al., 1982). Tethers appear to be a subset of membrane bound events since tethered beads could be pulled through the surface of the cell, indicating the absence of a (or a weak) cytoskeletal association.

As depicted in Fig. 3, locomoting WT cells displayed a significantly larger percentage of tethering at the cell uropod compared to the cell lamellipod ($P < 0.01$). In contrast to motile WT cells, nonmotile cells did not exhibit any spatial differences in tethering. Tether formation on untransfected motile 3T3 cells, which lack $\beta 1_c$ to which the mAb binds, is indicative of nonspecific associations. These data suggest that membrane deformability differs between the advancing and retracting portions of locomoting cells.

Migratory cells containing the $\beta 1$ integrin cytoplasmic domain truncation, 765t, displayed WT behavior for tether formation, with a significant difference between the retracting tail and the lamellipodium ($P < 0.004$). The fact that beads bound to 765t integrins, which cannot interact with the cytoskeleton, could readily exhibit tethers supports our hypothesis that tethers are a subset of membrane-attached events. In addition, the absolute levels of tethers are higher for 765t integrin compared with WT integrin since 765t integrin is unable to participate in cytoskeletal linkages and therefore has a higher probability of existing as tethers. The remainder of the integrin cytoplasmic domain mutants similarly had higher levels of tethering at the cell rear relative to that at the lamellipodium (data not shown). These results indicate that enhanced tethering at the cell rear does not involve an integrin-cytoskeletal interaction and is most likely a general characteristic of the membrane of moving cells.

Small Gold Aggregates Bound to Integrin Display Rapid, Intermittent, Motions Directed Preferentially to a Cell Edge

In addition to using the laser trap to test the associations of integrin with the cytoskeleton, we also monitored the dynamics of integrin-bound beads on the surfaces of motile and stationary cells. Previous work has demonstrated that integrin is transported forward on the dorsal surfaces of migrating fibroblasts after dispersion of contacts at the cell rear (Regen and Horwitz, 1992). However, little is known about the directed character, regulation, and cytoskeletal associations of the surface transport. We used nanometer-tracking of anti-$\beta 1_c$ mAb-coated gold particles on mouse fibroblasts transfected with chicken $\beta 1$ integrin constructs to examine the role of cytoskeletal interactions in surface transport of integrin.

Gold particles tagged with anti-$\beta 1_c$ integrin mAbs were allowed to interact with the dorsal surface of migrating cells. Individual beads and small aggregates of beads (aggregate diameter <260 nm, the limit of resolution of the microscope) were tracked on the lamellipodia of migrating cells for 90 s using video microscopy and image analysis techniques. Displacements of beads for the total tracking time were compared with those predicted for pure diffusion using a statistical analysis as described in Materials and Methods. A particle track with a low probability [$P(x) < 0.05$] that diffusion could give rise to the displacement of the bead is considered a directed event. In other words, some additional force is necessary to cause the integrin to move such a large distance. In addition, parallel MSD plots corresponding to each bead trajectory yielded information on the dynamic surface transport of integrins. A linear relationship between MSD and time is indicative of pure diffusion, while a nonlinear curve with a positive deviation suggests the presence of an external velocity component.

Dynamic gold bead behavior on the lamellipodial surfaces of migrating 3T3 WT cells was characterized by either diffusive motion or by brief periods of directed transport followed by diffusion (Fig. 4). When the paths of the particles are traced, they show distinct directed translocations or "jumps" (average velocity 37 ± 15 μm/min) (SD, $n = 34$) predominantly towards the edge (Fig. 4 C) although some are along the cell edge (Fig. 4 A). Since movements were also diffusive we used MSD versus time plots to analyze the directed versus diffusive components of movements along the major axis of displacement (data were fit to MSD = $2Dt$ + $(vt)^2$, where D is the apparent diffusion coefficient, v is the apparent velocity and t is the time). Pure diffusion as judged by $P(x) \geq 0.05$ and a straight line MSD plot ($v = 0$) was seldom seen with WT integrin although when observed (Fig. 4 B) the high average diffusion coefficient (2 × 10^{-10} cm^2/s) indicated that there was no restriction of diffusion. The apparent velocity ($v = 5$ μm/min) was lower than the instantaneous jump velocity because it represented a time averaged value. For migrating WT cells, 60 ± 13% of the tracked beads underwent directed transport, as determined from statistical analysis and MSD plots.

Intermittent, rapid movements often resulted in the transport of the gold bead to the edge of the cell, where the bead resumed diffusive motion restricted exclusively along the cell edge or along filopodial protrusions (Fig. 5). For WT cells, 67% of the beads undergoing directed motion were transported to the cell periphery. Side and forward leading edges were equally frequented by beads. Once a bead was caught at the edge, it remained there 15 to 60 s before it left the cell perimeter. In most cases, beads would interact multiple times with the same cell edge. For WT and 765t cells, ~50% of all beads displaying both diffusive and directed motions were observed to be caught at the cell edge for at least 15 s.

The restricted motion along the cell edge suggested an imposed restraining force. This possibility was explored by comparing the actual frequency for cell edge association with that predicted for diffusion alone. For our analysis, the bead was allowed to move small distances (up to 250 nm) from the cell boundary and still be considered restrained to the edge. The probability for a purely diffusing bead to be within 250 nm of the cell edge after 1 s is the result of integrating $P(x)dx = 1/(4\pi Dt)^{1/2}\exp(-x^2/4Dt)dx$ (Berg, 1983) for $x = 0$ to 250 nm and $t = 1$ s. A reflective boundary condition, $dP/dx = 0$ at $x = 0$, to account for the presence of the cell edge and the average value for diffusivity, 3 × 10^{-10} cm^2/s, were used in the calculation. This yields a probability of less than 0.7 that a bead would be found within 250 nm from the cell edge after 1 s. For a diffusing bead to remain constrained consecutively to the cell edge for 15 s, the proba-
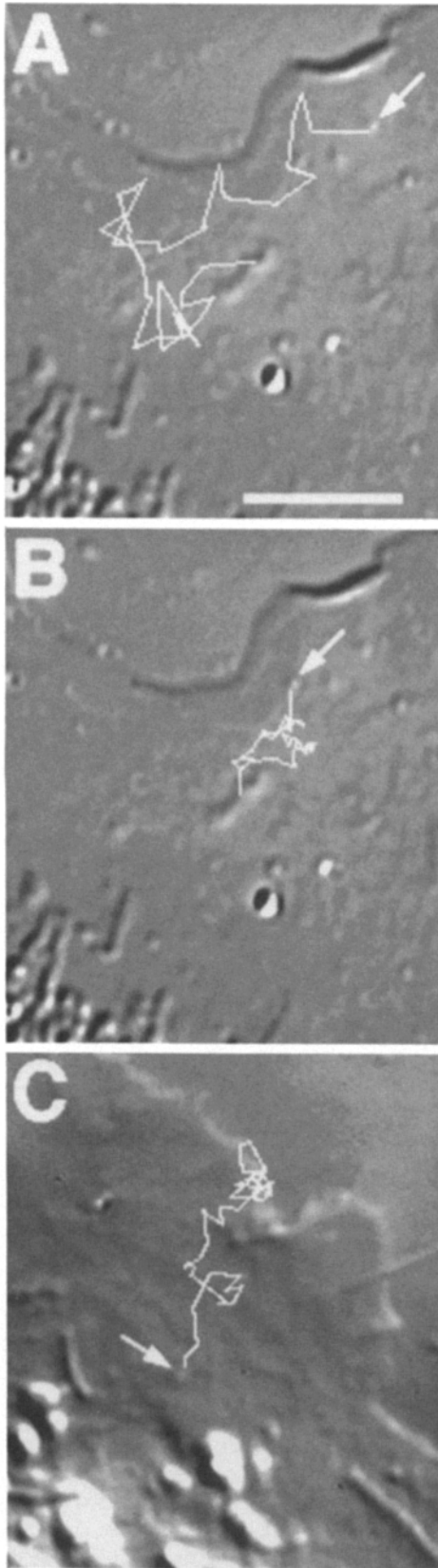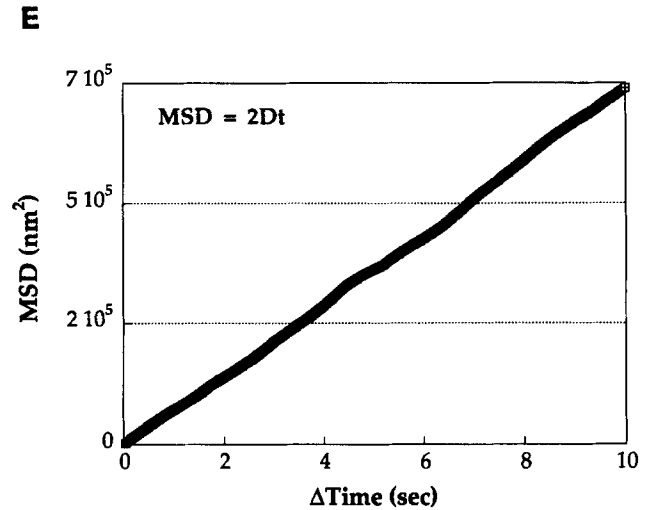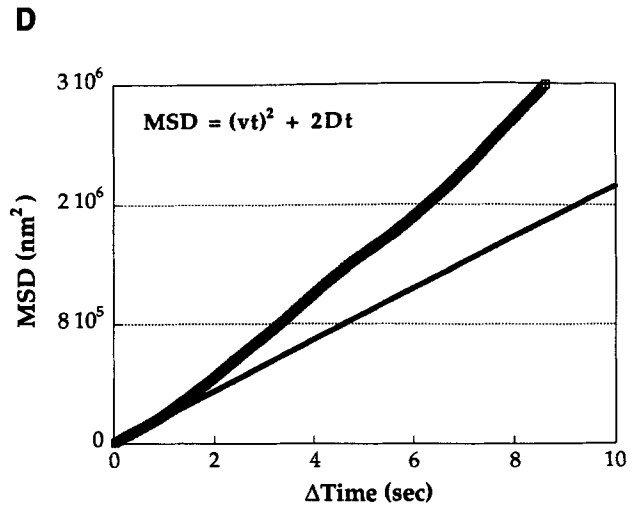
D

$$MSD = (vt)^2 + 2Dt$$

E

$$MSD = 2Dt$$

Figure 4. Integrin undergoes both directed and diffusive motions on the surfaces of 3T3 cells. 40-nm gold beads coated with ES66 (anti-$\beta1_c$ integrin mAb) were allowed to interact with the surfaces of migrating WT cells. Image analysis techniques were used to track the beads, yielding spatial position coordinates for the bead posi-

tion as a function of time. MSD plots of these paths as well as a statistical determination of the probability, $P(x)$, that the particular bead diffused a displacement x were used to distinguish diffusion from directed behavior. Particles with a low probability [$P(x)$ < 0.05] that their displacement was caused by pure diffusion are classified as undergoing directed transport. The arrows in A, B, and C indicate the initial positions of gold beads and the line sketches delineate the paths of the particles tracked for a total of 90 s at 2 s intervals. In A, the bead moves inward and along the cell lamellipodium in a series of directed [$P(x)$ = 0.01] and diffusive steps. In B, a different bead on the same cell undergoes pure diffusion [$P(x)$ = 0.3], and has no significant net displacement. In C, a bead on a different cell moves to the cell edge in a series of diffusive and directed steps [$P(x)$ = 0.02]. Of the beads undergoing directed transport on WT cells, 67% moved toward the cell periphery as illustrated in C. Plots of parallel MSD vs. time interval for the particles in A and B are shown in D and E, respectively. In D, the upward curvature indicates that a directed velocity exists, i.e., integrin is moving farther than predicted by pure diffusion (lower straight line). Fitting MSD = $2Dt$ + $(vt)^2$ to the data in B results in parameter values such that the $(vt)^2$ term is negligible (<10%) (E). Fits of the data as described in Materials and Methods yields v = 5 μm/min and D = 9 × 10^{-10} cm²/s for the directed particle (A). A value of D = 2 × 10^{-10} cm²/s is determined for B. Bar, 5 μm.
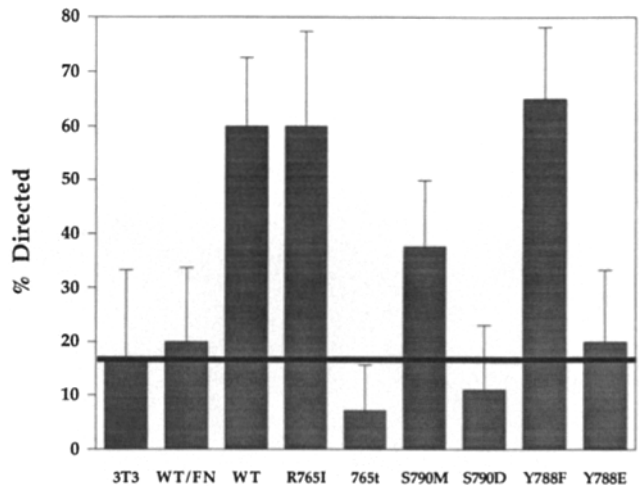
Figure 6. Intermittent, rapid transport requires sequences in the β1 integrin cytoplasmic domain. 40-nm-diameter gold beads coated with anti-β1c mAb were allowed to interact with the surfaces of migrating 3T3 β1 integrin transfectants. 10–16 beads were tracked using image analysis techniques on the lamellipodial surfaces of each cell type. The directed vs. diffusive behavior for each bead was determined from statistical analysis and MSD vs. time plots. The percentage of beads that underwent directed transport on each cell type is shown. WT, R765I, S790M, and Y788F integrin all displayed similar levels of directed transport on the surfaces of migratory cells. On the other hand, gold beads on motile 765t, S790D, and Y788E cells as well as beads on nonmotile WT cells (WT/FN), did not differ significantly from nonspecific behavior on untransfected 3T3 cells (the *black line* is a visual representation of the background levels for directed events). The error bars represent standard deviations calculated for proportions as described in Materials and Methods. These results indicate that rapid, intermittent motions of integrin require sequences in the β1 cytoplasmic domain.

Figure 5. Intermittent, rapid transport of integrin occurs preferentially to the cell periphery, where integrin resumes diffusion restricted along the edge. 40-nm gold beads coated with anti-β1c mAb (ES66) were allowed to interact with the surfaces of migrating WT cells. Beads exhibiting directed transport on the cell lamellipod were monitored for encounters with the cell edge. As pictured, the 40-nm gold bead coated with ES66 (*arrow*) moves to the cell edge where it diffuses exclusively along the edge for almost a minute. In the last frame, the bead eventually leaves the cell periphery. For this particular bead, as was often the case, the bead actually made

bility is $P = (0.7)^{15} = 4 \times 10^{-3}$. Thus, pure diffusion predicts an exceedingly low probability that a bead would stay within close proximity to the cell edge, compared with the observed 50%. These results imply that the restraint of integrin to the cell periphery is probably an active process and not a result of diffusion alone. However, the observation that 765t as well as WT integrin were capable of being restricted to diffuse along the cell edge indicates that such restriction does not require the cytoplasmic domain of β1 integrin.

Intermittent Motions on Motile Cells Require Sequences in the β1 Cytoplasmic Domain

The movements of small anti-β1c integrin mAb-coated gold particles were also monitored for nonmotile WT cells as well as for the various β1c integrin transfectants (Fig. 6). The data are presented as the number of beads displaying directed motion relative to the total number of beads monitored. Only 20 ± 14% of beads were intermittently transported on nonmotile WT cells. This value is significantly (P

multiple, lengthy encounters with the cell edge. Of the beads displaying directed behavior on the surface of 3T3 WT cells, 67% made extensive encounters of at least 15 s with the cell perimeter. Bar, 3 μm.
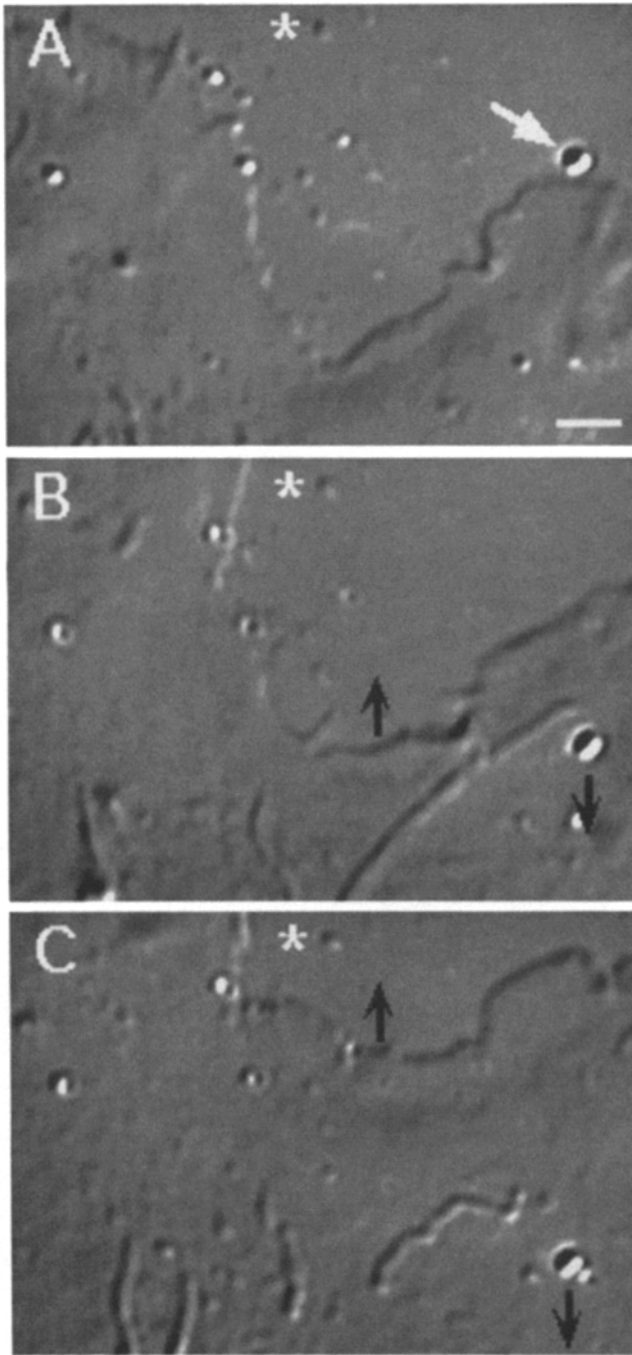
Figure 7 Rearward flow of a large aggregate of gold beads coated with anti-$\beta1_c$ integrin mAb on the front surface of a migrating 3T3 WT cell. 40-nm gold beads coated with the anti-$\beta1_c$ ES66 mAb were allowed to interact with the surfaces of migrating WT transfectants. Large aggregates of gold beads were monitored for movement on the front lamella of locomoting cells and the position of each aggregate was determined from images as a function of time. Images are shown at relative times of (*A*) 0, (*B*) 2, (*C*) 3, and (*D*) 5 min. The larger white arrow points to the gold aggregate and the asterisk marks a stationary particle on the coverslip. Smaller black arrows indicate the direction of advancement of the membrane and the movement of the gold aggregate. The lamellar region of the cell is at the top of each image and the nuclear region is toward the bottom portion of each photograph. Over time, the aggregate moves slowly and steadily toward the nuclear region, with little to no

< 0.05) lower than the percentage of directed beads on motile WT cells (60 ± 13%) and is not statistically distinct from levels of nonspecific directed motions of ES66-coated gold on untransfected 3T3 cells. These results suggest that directed transport, predominantly to cell edges, is characteristic of locomoting cells.

The dynamics of integrin on the surfaces of cells transfected with various integrin mutants were explored to clarify the role of cytoskeletal associations in these directed behaviors. There is a correlation between localization in focal adhesions (Reszka et al., 1992) and the probability of directed transport, indicating a requirement for the integrin cytoplasmic domain. For three integrins exhibiting normal focal contact localization (WT, R765I, Y788F), the probability of directed transport was approximately 60%. In contrast, the 765t truncation mutant exhibited only 7 ± 9% directed behavior, which is statistically lower than WT behavior ($P < 0.003$) but not distinct from nonspecific background (3T3). Directed transport of other integrins showing impaired focal contact localization (S790D, Y788E) was similarly reduced compared to WT ($P < 0.05$) yet also indistinguishable from nonspecific background levels.

As described for the latex bead trapping assay, the S790M mutant (which also exhibits normal focal contact localization) showed partial impairment of directed transport, with only 38 ± 12% of tracked particles undergoing such motions. This is still significantly higher than directed transport for the 765t mutant ($P < 0.05$), and is statistically indistinguishable from WT behavior to $P < 0.05$. Again, this may reflect the nonconservative nature of this substitution as well as differences between the two assays and the phenomena they probe.

Beads that exhibited rapid transport on WT and mutant cells had velocities that did not differ substantially from one another and averaged 3.8 ± 1.4 μm/min (SD, $n = 25$). Recall that beads undergoing directed transport are characterized by periods of either pure diffusion, steady directed motion combined with a diffusive component, and/or rapid jumps with a negligible diffusive element. Our fit of the data to the second order polynomial MSD = $2Dt + (vt)^2$ (parallel MSD) resulted in an average value for v, assuming a constant velocity imposed on the particle. The instantaneous velocities of individual bead jumps were about an order of magnitude higher ($v_i = 37 ± 15$ μm/min) (SD, $n = 34$) than the average velocities extracted from MSD plots.

Diffusivities for beads on WT and mutant cells averaged 2.9 ± 2.1 × 10^{-10} cm^2/s (SD, $n = 84$). There were no significant differences in diffusivities among the various mutant integrins (e.g., $D = 3.6 ± 3.3 × 10^{-10}$ cm^2/s for WT and $D = 3.4 ± 2.3 × 10^{-10}$ cm^2/s for 765t) nor between beads undergoing pure diffusion versus beads intermittently transported. Our values are consistent with Sheetz et al. (1989) who reported a diffusivity of 10^{-10} to $3 × 10^{-9}$ cm^2/s for randomly moving particles, and Kucik et al. (1989) who found that ConA-coated particles undergoing rapid, forward

diffusive component. The average velocity for rearward flow of large aggregates is 0.85 ± 0.44 (SD, $n = 54$) μm/min, relative to the substrate, and the average aggregate diameter is 1.4 ± 0.4 μm. Bar, 2 μm.

transport had diffusion coefficients in the range of 10^{-10} to 10^{-9} cm^2/s.

Large Gold Aggregates Bound to Integrin Move Slowly and Steadily Rearward

In contrast to the intermittent, rapid transport of small gold aggregates (<260 nm in diameter), large aggregates of 40-nm gold beads (aggregate diameter of 1.4 ± 0.4 μm) coated with the ES66 mAb moved steadily rearward on the lamella of 3T3 WT fibroblasts. Representative images are shown in Fig. 7 at times between 0 and 5 min. The larger white arrow points to the gold aggregate and the asterisk marks a stationary particle on the coverslip. Smaller black arrows indicate the direction of advancement of the membrane and the movement of the gold aggregate.

The rearward flow was continuous, without an obvious diffusive component. This type of transport is identical to the centripetal flow of latex beads coated with an anti-integrin mAb observed after cytoskeletal linkage was induced using the laser optical trap. The average rate of rearward motion for aggregates of WT and various mutant integrins was 0.85 ± 0.44 μm/min (SD, $n = 54$) relative to the substratum, which is significantly ($P < 10^{-15}$) lower than the time-averaged velocity for rapid, intermittent transport, 3.8 ± 1.4 μm/min, and is much lower than the instantaneous jump velocity, 37 ± 15 μm/min. The average velocity for rearward transport relative to the leading edge is approximately twice the velocity relative to the substratum.

Discussion

Cell migration is a phenomenon requiring dynamic adhesive interactions between the internal motile machinery and the external substratum, with adhesion receptors such as integrins serving as the transmembrane link. Two questions which have arisen are (a) Is there an asymmetry in the adhesive interactions at the cell lamellipodium compared with the cell rear? and, (b) How is integrin supplied to areas of new adhesive contacts? To explore these questions, we used laser optical trapping and nanometer-precision motion analysis to investigate integrin cytoskeletal associations at the cell lamellipodium and retracting tail and to monitor the surface dynamics of $\beta 1$ integrin, respectively. The following observations were made: (a) integrin binds to the cytoskeleton more readily at the lamellipodium versus the rear of a migrating cell, whereas stationary cells do not exhibit such differential binding; (b) the membrane of motile cells is significantly more deformable at the cell rear compared with the cell lamellipodium, as evidenced by the ability to stretch the cell membrane with the laser trap; (c) integrin bound by small aggregates of gold particles displays rapid, intermittent motions directed preferentially to a cell edge; (d) integrin cross-linked by large aggregates of anti-integrin mAb-coated gold particles moves slowly and steadily rearward at a rate that corresponds closely to the rate of actin treadmilling; and (e) front/rear integrin cytoskeletal asymmetry and rapid directed transport of integrin, but not a highly deformable membrane at the cell rear, require sequence specific integrin–cytoskeleton interactions.

An asymmetry in cell-substrate interactions between the cell lamellipodium and cell rear could occur by several pos-sible mechanisms which include front vs. rear differences in cytoskeletal architecture and integrin–cytoskeletal linkages. We found that integrin does not form stable linkages with the cytoskeleton at the cell rear but does at the lamellipod, either reflecting differences in the intrinsic cytoskeletal architecture or alterations in the linkages themselves. An inability to form linkages at the cell rear could potentially arise from posttranslational modifications of the linkage proteins, including integrin. Phosphorylations of adhesion-associated proteins, e.g., tensin, FAK, and paxillin, are thought to be involved in stabilizing adhesive structures (Davis et al., 1991; Burridge et al., 1992). Therefore, de-phosphorylation of these proteins (or phosphorylation of other linkage proteins) may trigger release of cytoskeletal linkages at the cell rear. It is also possible that release of adhesions are mediated by phosphorylation of integrin. Several labs have reported that phosphorylation of both the tyrosine (788) and serine (790) residues on $\beta 1$ integrin negatively regulates the interaction of integrin with the cytoskeleton (Hirst et al., 1986; Dahl and Grabel, 1989; Horvath et al., 1990; Reszka et al., 1992). In our studies, $\beta 1$ integrin cytoplasmic domain mutants with these tyrosine and serine residues replaced with negatively charged residues (to mimic the phosphorylated states) have a drastically reduced ability to bind to the cytoskeleton. However, the absence of effects for the Y788F mutant and small effects for the S790M mutant (alterations such that the tyrosine and serine cannot be phosphorylated) question the role of these particular integrin phosphorylations during rear release.

We have also provided evidence that the cytoskeleton in the cell rear is not as well associated with the membrane, as indicated by the ability to stretch the membrane as tethers using the laser trap. We saw a similar deformability at the cell rear for cells containing the cytoplasmic domain truncation mutant indicating that integrin in tethers does not interact with the cytoskeleton.

A deformable membrane at the cell rear and weakened adhesive linkages could possibly function together to generate spatial asymmetry in the traction exerted by the cell. We emphasize that both sources of asymmetry exist only in locomoting cells, since nonmotile cells do not exhibit spatial differences in integrin cytoskeletal associations or in membrane deformability. This hypothesis is also supported by the work of Regen and Horwitz (1992) who showed that integrin-mediated adhesive contacts between the cell and substratum are released at the cell rear by two modes. A portion of the integrin appears to disperse from adhesive contacts and be transported on the dorsal surface to the cell front, while another portion of the integrin remains aggregated in adhesive contacts. These contacts are "ripped" from the cell body, leaving integrin and membrane, but no cytoskeletal proteins, associated with substrate as tracks behind the moving cell. Thus, it appears that a loose, less structured (deformable) membrane helps the cell to advance by leaving a portion of its contacts behind. The release of contacts by a ripping mechanism appears to be accompanied by a regulated uncoupling of the integrin–cytoskeleton bond since cytoskeletal proteins were not found in the cell tracks. Our finding of an asymmetric integrin–cytoskeleton association that is sensitive to modifications of the integrin cytoplasmic domain suggest that a regulated uncoupling at the cell rear could occur.

The observation of two distinct surface behaviors for integrin bound by colloidal gold, a slow centripetal motion and an intermittent rapid transport combined with diffusion, imply the existence of multiple linkages of integrin to the cytoskeleton. The slower rearward flow likely represents a stable linkage of large aggregates of cross-linked integrin, as described for other cross-linked surface proteins, to rearward flowing cortical actin. This phenomena is identical to the capping of general surface proteins observed in other systems (Harris and Dunn, 1972; Dembo and Harris, 1981; Fisher et al., 1988). The rate of slow, rearward flow, $v = 0.85 \pm 0.44$ μm/min relative to the substrate, corresponds closely to the velocity for cortical actin flow, 0.79 μm/min (Wang, 1985), supporting a proposed linkage of the integrin to the actin.

Since the rate of stable centripetal protein transport ($v = 0.85$ μm/min) on the dorsal surface is within the same order of magnitude as fibroblast locomotion under our conditions, $v = 0.5 - 1$ μm/min (our unpublished observations; Regen and Horwitz, 1992), rearward movement of ventral integrins adhered to a nondeformable substrate could possibly account for the locomotion of these cells. This is consistent with the hypothesis that transmembrane proteins bind to the underlying moving cytoskeleton, which in turn drives particle flow on the cell surface (Sheetz et al., 1989; Kucik et al., 1990; Lee et al., 1990). The relevance of studying dorsal events to infer information on the ventral side of the cell is supported by Harris and Dunn (1972) who demonstrated that particles adhered to dorsal and ventral surfaces of migrating fibroblasts move centripetally rearward at comparable speeds. These data suggest that there are no differences in surface protein–cytoskeleton interactions at the cell top compared to the bottom. Also, Mueller et al. (1989) found that suspended cells responded to immobilized fibronectin (presented using latex spheres) by organizing integrin and talin to the site of bead contact. Such organization is similar to that found in focal contact-like structures on the ventral side of the cell, indicating that cells respond to a small "surface" similarly to how they respond to the underlying immobilized substrate. In vivo, and in three-dimensional matrices, cells are surrounded on all sides by a substrate. Therefore, the motile cell has no intrinsic dorsal–ventral distinction and may be predicted to behave similarly over its entire surface in the event that the cell encounters substrate from any "side."

The faster, intermittent transport behavior of small aggregates of integrin seems to be driven by cytoskeletal interactions, since directed transport is not observed when the integrin cytoplasmic domain is truncated. Directed transport consists of periods of "jumps," with an instantaneous velocity of 37 μm/min, followed by either pure diffusion or diffusion with an imposed velocity, suggesting that integrin interacts transiently with moving cytoskeletal elements. Such transport is possibly mediated by a motor protein, since forward motions toward the barbed end of actin are observed, and may be used to transport integrin to existing and newly formed edges of migrating cells where new adhesive contacts are nucleated (Kucik et al., 1989; Regen and Horwitz, 1992). This transport is likely not a result of unusual diffusion patterns since in the laser optical trapping experiments for WT integrin we were able to pull membrane bound beads through the membrane without restriction. In addition, Edidin et al. (1991) demonstrated that cytoplasmic barriers to diffusion are large (0.6–1.7 μm) compared with the distance traversed by diffusing and transported integrins. These data indicate that "domains" or barriers to diffusion likely do not play a large role in generating the observed rapid, directed transport characteristics.

These fast, intermittent motions are similar to the forward transport of 40-nm ConA-coated gold beads observed on the dorsal surfaces of migrating fish epidermal keratocytes (Kucik et al., 1989) and neurons (Sheetz et al., 1990). In contrast to ConA on fish keratocytes, integrin is transported on the surfaces of mouse fibroblasts both forward and rearward, with a preference toward side and front edges of the cell (67% for WT). We speculate that rapid and highly directed cells such as the keratocytes, which move at a rate of 30 μm/min, require that proteins be supplied exclusively to the forward leading edge. However, slow moving fibroblasts frequently change spreading and retracting regions during the locomotion process. Therefore, the supply of integrin to front and side edges is quite appropriate for these "indecisive" cells. These rapid, directed motions probably involve interactions between linkage proteins and the integrin cytoplasmic domain since mutations that mimic the phosphorylation of either tyrosine or serine residues (Y788E or S790D) inhibit the directed transport of these integrins.

Once transported to the cell edge, integrin is trapped by the curved region at the cell periphery and transiently diffuses along the cell edge and along filopodial protrusions. The restricted motion of integrin along cell edges, ruffles, or filopodia appears to be an active process since pure diffusion predicts a much shorter time for a random edge encounter. Sheetz et al. (1990) similarly observed "dynamic trapping" of the 2A1 antigen at the edges of neuronal growth cones. They speculated that the particles were either attached to cytoplasmic components moving along the edges or that particle diffusion was restrained by barriers running parallel to the periphery. We observed edge restraint for directed and diffusing WT and 765t integrins at cell edges which suggests that dynamic trapping of integrin in motile fibroblasts does not involve specific β1 integrin–cytoskeletal associations. Cytoskeletal barriers running parallel to the cell periphery or the membrane curvature might act to physically or energetically restrain diffusion along the edge. Recall that 765t integrin, although lacking the β1 cytoplasmic domain, contains an intact α subunit that could be restrained by physical means. However, no known cytoskeletal proteins bind specifically to the α subunit of integrin. Most likely, the curvature of the membrane restrains diffusion to cell edges, filopodia, and ruffles, since Edidin et al. (1991) demonstrated that cytoplasmic barriers to diffusion are large (0.6–1.7 μm) in comparison with the areas of restraint observed for edge entrapment. Irrespective of the mechanism for dynamic trapping, this process of maintaining integrin at the cell periphery likely enhances the probability that integrin will make contact with the substratum and nucleate the nascent adhesive contacts which are forming there.

This transport of integrin to the cell periphery where new contacts form is consistent with findings of Regen and Horwitz (1992). They used live-cell immunofluorescent staining of integrin to show that integrin-mediated contacts form at the cell's leading edge. These contacts remain stationary with respect to the substratum and are initially very faint

then grow in size and intensity as the cell moves over them. However, Regen and Horwitz (1992) did not observe a build-up of integrins on the cell's leading edge; in fact, they observed a relative depletion of integrins at the cell front. An accumulation of integrins at the cell edge is not observed since the concentration of integrins in this region depends on the dynamic balance between movement toward and movement away from the leading edge. The "edge restraint" that we observed for integrin occurred for only 15–60 s. In other words, integrins were not indefinitely trapped at the leading edge, but their restriction along the edge was longer than that

A. Cell Front
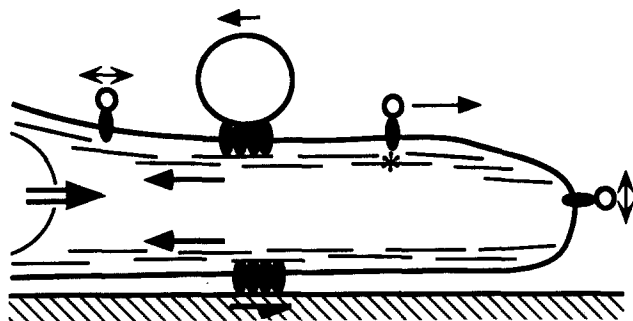
B. Cell Rear
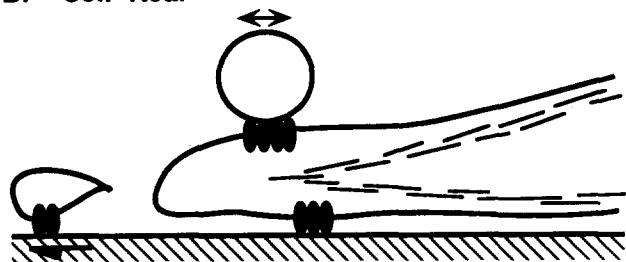
Figure 8. Model for integrin dynamics in cell migration. Cyto-skeletal stresses (indicated by ◄——) exert an inward centripetal force on attached integrin (●). If integrin is not associated with the substrate, it and the attached latex bead will be pulled inward (indicated by ◄——) at rate similar to that for actin flux (∼0.8 μm/min). Integrin that is linked to the substrate will withstand being pulled inward, leading to a resisting force exerted on the cell (——►). A front-to-rear asymmetry in adhesive contacts would lead to an asymmetry in the resisting forces exerted on the cell, and hence, net movement of the rest of the cell forward (══►). An asymmetry in adhesive interactions could potentially be generated by selective phosphorylation of integrin at the cell rear that enhances the dissociation of integrin from the cytoskeleton. The cytoskeleton appears to interact more weakly with the membrane in the back of the cell resulting in a more deformable membrane. This in turn may allow adhesive contacts not linked to the cyto-skeleton to break free from the cell body at the cell rear. Integrin bound by small gold particles on the dorsal surface can either diffuse (◄►) with a diffusivity of ∼3 × 10⁻¹⁰ cm²/s or be directed rapidly ($v = 4 - 40$ μm/min) to cell edges (——►). This rapid directed motion may be mediated by motor proteins (*) and may be necessary to supply integrin to advancing portions of the cells where new contacts are formed.

predicted for pure diffusion. At the same time, there is also movement of integrins away from the cell edge (cell frame of reference) due to accumulation into adhesive "macroaggregates" which remain fixed to the substratum (Regen and Horwitz, 1992). These aggregates are faint when first formed then grow in size and intensity as the cell moves forward. In effect, the integrins are transported away from the front.

In light of our new findings, we offer Fig. 8 as a schematic illustration of a current working model for integrin dynamics in migrating fibroblasts. On the cell lamellipodium, integrins are transported preferentially to the leading edge where they can participate in the formation of nascent adhesion macro-aggregates by binding substratum ligands. These macroaggregates grow as they accumulate integrins and become associated with an intracellular motor that exerts a rearward force on them. On the dorsal surface macroaggregates are thus drawn rearward while on the ventral surface they remain fixed to the substratum permitting intracellular components to be drawn forward. Toward the cell rear, the linkages between integrins in macroaggregates and the cytoskeleton uncouple, thus weakening the connection between the cytoskeleton and the substratum. Decoupled macroaggregates that find themselves in regions of deformable membrane at the cell rear are susceptible to ripping. Other decoupled macro-aggregates may disperse, facilitating dissociation of integrin/ substratum-ligand bonds. Overall, this scheme of integrin dynamics allows for continual transport of adhesion receptors to the cell's leading edge, into adhesion structures, to the cell rear (moving with respect to the cell frame-of-reference but fixed with respect to the substratum), and out of adhesion structures. At the same time, the asymmetry in linkages provides a mechanism for directional cell migration.

References

Abercrombie, M., J. E. M. Heaysman, and S. M. Pegrum. 1970. The locomotion of fibroblasts in culture. III. Movements of particles on the dorsal surface of the leading lamella. *Exp. Cell Res.* 62:389–398.

Albelda, S. M., and C. A. Buck. 1990. Integrins and other cell adhesion molecules. *FASEB (Fed. Am. Soc. Exp. Biol.) J.* 4:2868–2880.

Ashkin, A., and J. M. Dziedzic. 1989. Internal cell manipulation using infrared laser traps. *Proc. Natl. Acad. Sci. USA.* 86:7914–7918.

Ashkin, A., J. M. Dziedzic, and T. Yamane. 1987. Optical trapping and manipulation of single cells using infrared-laser beams. *Nature (Lond.).* 330:769–771.

Berg, H. C. 1983. Random Walks in Biology. Princeton University Press, Princeton, NJ. 14–16.

Bershadsky, A. D., and J. M. Vasiliev. 1988. Cytoskeleton. Plenum Press, New York. 217–250.

Bray, D. 1970. Surface movements during the growth of single explanted neurons. *Proc. Natl. Acad. Sci. USA.* 65:905–910.

Bretscher, M. S. 1976. Directed lipid flow in cell membranes. *Nature (Lond.).* 260:21–23.

Buck, C. A., and A. F. Horwitz. 1987. Cell surface receptors for extracellular

matrix molecules. *Annu. Rev. Cell Biol.* 3:179–205.

Burridge, K., K. Faith, T. Kelly, G. Nuckolls, and C. Turner. 1988. Focal adhesions: transmembrane junctions between the extracellular matrix and the cytoskeleton. *Annu. Rev. Cell Biol.* 4:487–525.

Burridge, K., C. E. Turner, and L. H. Romer. 1992. Tyrosine phosphorylation of paxillin and pp125^{FAK} accompanies cell adhesion to extracellular matrix: a role in cytoskeletal assembly. *J. Cell Biol.* 119:893–903.

Croxton, F. E. 1953. Elementary Statistics with Applications in Medicine and the Biological Sciences. Dover Publications, Inc., New York. 259–265.

Dahl, S. C., and L. B. Grabel. 1989. Integrin phosphorylation is modulated during the differentiation of F-9 teratocarcinoma stem cells. *J. Cell Biol.* 108:183–190.

Davis, S., M. L. Lu, S. H. Lo, S. Lin, J. A. Butler, B. J. Druker, T. M. Roberts, Q. An, and L. B. Chen. 1991. Presence of an SH2 domain in the actin-binding protein tensin. *Science (Wash. DC).* 252:712–715.

Dembo, M., and A. Harris. 1981. Motion of particles adhering to the leading lamella of crawling cells. *J. Cell Biol.* 91:528–536.

DiMilla, P. A., K. Barbee, and D. A. Lauffenburger. 1991. Mathematical model for the effects of adhesion and mechanics on cell migration speed. *Biophys. J.* 60:15–37.

Duband, J.-L., G. H. Nuckolls, A. Ishihara, T. Hasegawa, K. M. Yamada, J. P. Thiery, and K. Jacobson. 1988. Fibronectin receptor exhibits high lateral mobility in embryonic locomoting cells but is immobile in focal contacts and fibrillar streaks in stationary cells. *J. Cell Biol.* 107:1385–1396.

Edidin, M., and A. Weiss. 1972. Antigen cap formation in cultured fibroblasts: a reflection of membrane fluidity and of cell motility. *Proc. Natl. Acad. Sci. USA.* 69:2456–2459.

Edidin, M., S. Kuo, and M. P. Sheetz. 1991. Lateral movements of membrane glycoproteins restricted by dynamic cytoplasmic barriers. *Science (Wash. DC).* 254:1379–1382.

Fisher, G. W., P. L. Conrad, R. L. DeBiasio, and D. L. Taylor. 1988. Centripetal transport of cytoplasm, actin and the cell surface in lamellipodia of fibroblasts. *Cell Motil. Cytoskeleton.* 11:235–247.

Gelles, J., B. J. Schnapp, and M. P. Sheetz. 1988. Tracking kinesin-driven movements with nanometre-scale precision. *Nature (Lond.).* 331:450–453.

Harris, A., and G. Dunn. 1972. Centripetal transport of attached particles on both surfaces of moving fibroblasts. *Exp. Cell Res.* 73:519–523.

Hayashi, Y., B. Haimovich, A. Reszka, D. Boettiger, and A. Horwitz. 1990. Expression and function of chicken integrin β1 subunits and its cytoplasmic domain mutants in mouse NIH 3T3 cells. *J. Cell Biol.* 110:175–184.

Heidemann, S. R., P. Lamoureux, and R. E. Buxbaum. 1990. Growth cone behavior and production of traction force. *J. Cell Biol.* 111:1949–1957.

Hirst, R., A. Horwitz, C. Buck, and L. R. Rohrschneider. 1986. Phosphorylation of the fibronectin receptor complex in cells transformed by oncogenes that encode tyrosine kinases. *Proc. Natl. Acad. Sci. USA.* 83:6470–6474.

Hochmuth, R. M., H. C. Wiles, E. A. Evans, and J. T. McCown. 1982. Extensional flow of erythrocyte membrane from cell body to elastic tether: II. Experiment. *Biophys. J.* 39:83–89.

Horvath, A. R., M. A. Elmore, and S. Kellie. 1990. Differential tyrosine-specific phosphorylation of integrin in Rous sarcoma virus transformed cells with differing transformed phenotypes. *Oncogene.* 5:1349–1357.

Horwitz, A., K. Duggan, C. Buck, M. C. Beckerle, and K. Burridge. 1986. Interaction of plasma membrane fibronectin receptor with talin—a transmembrane linkage. *Nature (Lond.).* 320:531–532.

Hynes, R. O. 1987. Integrins: a family of cell surface receptors. *Cell.* 48:549–554.

Kucik, D. F., E. L. Elson, and M. P. Sheetz. 1989. Forward transport of glycoproteins on leading lamellipodia in locomoting cells. *Nature (Lond.).* 340:315–317.

Kucik, D. F., E. L. Elson, and M. P. Sheetz. 1990. Cell migration does not produce membrane flow. *J. Cell Biol.* 111:1617–1622.

Kucik, D. F., S. C. Kuo, E. L. Elson, and M. P. Sheetz. 1991. Preferential attachment of membrane glycoproteins to the cytoskeleton at the leading edge of lamella. *J. Cell Biol.* 114:1029–1036.

Kuo, S. C., J. Gelles, E. Steuer, and M. P. Sheetz. 1991. A model for kinesin movement from nanometer-level measurements of kinesin and cytoplasmic dynein and force measurements. *J. Cell Sci.* 14:135–138.

Lackie, J. M. 1986. Cell Movement and Cell Behavior. Allen and Unwin, Inc., Winchester, MA. 155–168.

LaFlamme, S. E., S. K. Akiyama, and K. M. Yamada. 1992. Regulation of fibronectin receptor distribution. *J. Cell Biol.* 117:437–447.

Lee, J., M. Gustafsson, K. E. Magnusson, and K. Jacobson. 1990. The direction of membrane flow in locomoting polymorphonuclear leukocytes. *Science (Wash. DC).* 247:1229–1233.

Mueller, S. C., T. Kelly, M. Dai, H. Dai, and W.-T. Chen. 1989. Dynamic cytoskeletal-integrin associations induced by cell binding to immobilized fibronectin. *J. Cell Biol.* 109:3455–3464.

Otey, C. A., F. M. Pavalko, and K. Burridge. 1990. An interaction between a-actinin and the β1 integrin subunit in vitro. *J. Cell Biol.* 111:721–729.

Regen, C. M., and A. F. Horwitz. 1992. Dynamics of b1 integrin-mediated adhesive contacts in motile fibroblasts. *J. Cell Biol.* 119:1347–1359.

Reszka, A. R., Y. Hayashi, and A. F. Horwitz. 1992. Identification of amino acid sequences in the integrin β1 cytoplasmic domain implicated in cytoskeletal association. *J. Cell Biol.* 117:1321–1330.

Ruoslahti, E., and M. D. Pierschbacher. 1987. New perspectives in cell adhesion: RGD and integrins. *Science (Wash. DC).* 238:491–497.

Ruoslahti, E., E. G. Hayman, M. Pierschbacher, and E. Engvall. 1982. Fibronectin: purification, immunochemical properties, and biological activities. *Methods Enzymol.* 82:803–831.

Rupert, T., H. Rohde, L. Risteli, U. Ott, P. G. Robey, and G. R. Martin. 1982. Laminin. *Methods Enzymol.* 82:831–837.

Sheetz, M. P., S. Turney, H. Qian, and E. L. Elson. 1989. Nanometre-level analysis demonstrates that lipid flow does not drive membrane glycoprotein movements. *Nature (Lond.).* 340:284–288.

Sheetz, M. P., N. L. Baumrind, D. B. Wayne, and A. L. Pearlman. 1990. Concentration of membrane antigens by forward transport and trapping in neuronal growth cones. *Cell.* 61:231–241.

Singer, S. J., and A. Kupfer. 1986. The directed migration of eukaryotic cells. *Annu. Rev. Cell Biol.* 2:337–365.

Solowska, J., J.-L. Guan, E. E. Marcantonio, J. E. Trevithick, C. A. Buck, and R. O. Hynes. 1989. Expression of normal and mutant avian integrin subunits in rodent cells. *J. Cell Biol.* 109:853–861.

Tapley, P., A. Horwitz, C. Buck, K. Burridge, K. Duggan, and L. Rohrschneider. 1989. Integrins isolated from rous sarcoma virus-transformed chicken embryo fibroblasts. *Oncogene.* 4:325–333.

Trinkaus, J. P. 1984. Cells into Organs. The Forces that Shape the Embryo. Prentice-Hall, Inc., Englewood Cliffs, NJ. 187–226.

Wagner, S. F. 1992. Introduction to Statistics. HarperCollins Publishers, Inc., New York. 195–213.

Wang, J. 1985. Exchange of actin subunits at the leading edge of living fibroblasts: possible role of treadmilling. *J. Cell Biol.* 101:597–602.

Wang, N., J. P. Butler, and D. E. Ingber. 1993. Mechanotransduction across the cell surface and through the cytoskeleton. *Science (Wash. DC).* 260:1124–1127.

Waugh, R. E. 1982. Surface viscosity measurements from large bilayer vesicle tether formation: II. Experiments. *Biophys. J.* 38:29–37.